Computational Modelling of Flatfoot Deformity

Alves, M.
mariana.alves@tecnico.ulisboa.pt

Instituto Superior Técnico, Lisboa, Portugal

December 2020

Abstract: Flatfoot is a deformity that leads to the misalignment of the foot and ankle joints, affecting 25% of the general population. Despite being a common foot deformity, the biomechanics of flatfoot are not fully understood. Choosing the best suited surgical treatment to correct this deformity is a troubling subject among the medical community. This work is presented as a first approach, using finite element method for the evaluation of the biomechanical behaviour of the foot when its anatomy sets up in a valgus foot situation. A foot and ankle finite element model of both a healthy and a flatfoot were developed consisting of bones, cartilages, ligaments, and tendons. A comparison between the von Mises stresses distribution of the healthy and the flatfoot was performed. Overall, the results showed that the flatfoot was subjected to higher stresses than the healthy foot. The cartilages and ligaments of the flatfoot also yield higher stresses than the healthy foot. The clinical use of this type of FE models can be of great importance since they can lead the way for novel diagnostic techniques and novel methods for treatment planning/optimization. In the future, a study of which should be the most suitable osteotomy for flatfoot correction will be performed, using the model developed on this work.

Key words: Finite Element Method, Biomechanics, Flatfoot, Ligaments, Tendons

1. Introduction

Flatfoot or valgus foot is a multifactorial deformity that results from several changes of the foot anatomy, leading to a misalignment of the foot and ankle joints, affecting 25% of the general population. Such alterations cause pain and potentiate the alteration of the foot biomechanics. It can be easily understood that flatfoot is a pathology that strongly influences the quality of life, not only in a daily basis but also in terms of sports performance, since it increases injury risk. Moreover, recent studies demonstrate the existence of a greater propensity in developing other type of lower limb injuries in individuals with valgus foot [1].

Flatfoot deformity is a complex deformity associated with the progressive weakening of the tibialis posterior tendon (TPT) resulting in the collapse of the medial longitudinal arch [2],[3], since it is the main responsible for supporting the arch. Once TPT fails to function, pathologic forces transmitted through the midfoot result in transverse tarsal joint collapse and forefoot abduction. Furthermore, the force vector applied by the Achilles tendon becomes lateral relative to the centre of the subtalar joint, contributing to the valgus deformity seen in patients with valgus foot.

Although, valgus foot was originally described as tibialis posterior tendon dysfunction, it is now recognized to be a progressive deformity that involves many other structures [3]. So, this deformity is a combination of TPT insufficiency and failure of both capsular and ligamentous structures of the foot, which result in the combination of plantar sag, midfoot abduction and heel valgus [2], [4].

The main causative factor of flatfoot deformity is known to be TPT dysfunction but it has shown to be a multifactorial pathology with other factors contributing to its appearance or aggravation, such as increasing age, obesity, ligamentous laxity, trauma and systemic inflammatory conditions [4]. Additionally, tight gastrocnemius-soleus complex, posterior tendon hypovascularity, diabetes mellitus and hypertension can also contribute to the deformity [3].

Johnson and Storm were the first to suggest a classification system for this deformity. This system was a 3-stage system based on the condition of the TPT, hindfoot alignment and flexibility of the deformity. Years later, a fourth stage was added to this classification by Myerson (*Table 1)* for describing deltoid ligament insufficiency with valgus collapse and degeneration of the ankle.

For the diagnosis of the deformity, physical examination is the gold standard

To complement physical examination, the doctors commonly resort to medical imaging. Weight-bearing images seem to be very helpful in the classification of the deformity, allowing the doctor to measure several parameters to evaluate if the pathology is present. For the evaluation of the longitudinal arch, the Meary's angle, the calcaneal inclination angle and the calcaneal-5th metatarsal angle must be used. The most common metrics for hindfoot valgus and

Table 1 – Myerson Modification of Johnson and Storm Classification of Adult-Acquired Flatfoot Deformity (Adapted from [3])

Stage	Description
I	Mild medial pain and swelling with no deformity, can perform heel-rise test but demonstrates weakness on repetition, tenosynovities on pathology with normal tendon length
II	Moderate pain with or without lateral pain, flexible deformity, unable to perform heel-rise test, elongated tendon with longitudinal tears
IIA	<30% talar head uncoverage
IIB	>30% talar head uncoverage
III	Severe pain, fixed deformity, unable to perform heel-rise test, visible tears on pathology
IV	Lateral talar tilt
IVA	Flexible ankle valgus without severe arthritis
IVB	Fixed ankle valgus with or without severe arthritis

forefoot abduction are the talocalcaneal angle, talus-1st metatarsal axis and the talonavicular angle [5] .

MRI imaging has also been showed to have a high sensitivity and specificity for diagnosing adult acquired flatfoot deformity (AAFD), since it allows for a visualization of soft tissues.

For the treatment of AAFD two approaches can be taken: the non-operative management and the operative management. The non-operative management commonly is the first line of treatment for the flatfoot deformity, including immobilization, non-steroidal anti-inflammatory drugs, braces, orthotics and physical therapy [3]. In cases where non-operative modalities fail, operative intervention is warranted. The options for surgical treatment are defined by the stage of the deformity [4].

The wide variability of current available treatment alternatives, caused, in part, by a still latent lack of knowledge of certain biomechanical variables that have not been adequately evaluated by experimental trials, makes the choosing of the best suitable treatment for each patient a highly subjective process, based on the clinicians' empiric experience. For instance, choosing the best osteotomy, while providing an efficient and accurate restoration of the foot biomechanics and functions, has been a troubling subject amongst the medical community.

Having pointed such factors and constraints, this work is presented as a first approach, using Finite Element Method (FEM), for the evaluation of the biomechanical behaviour of the foot when its anatomy sets up in a deformed situation, in this case, the valgus foot. For that purpose, a finite element (FE) model of the foot and ankle with and without deformity is developed to compare the biomechanics of both situations. The development of FE models that are clinically applicable can be of great use in clinical practice once they can lead the way or novel diagnostic techniques and novel methods for treatment planning/optimization.

2. Background

The first biomechanical evaluations of foot function were performed in cadaveric models. From these studies, important information regarding the biomechanics effects of tendons, ligaments and plantar fascia were taken. However, cadaver studies require high financial investments in measurement equipment, as well as a meticulous control over the study samples that guarantees the biomechanical characteristics of the tissue [6]. Moreover, some limitations have been identified, especially when dealing with a certain kind of pathologies which is the case of AAFD. Due to the lack of foot donors, healthy foot samples have been frequently used to artificially create flatfoot deformities by realising or sectioning ligaments and tendons. However, clinical flatfoot functions are not fully reproduced through these artificial flatfoot samples since they are both patient- and stage-dependent [7]. Limitations of the measurement techniques lead to difficulties obtaining the detailed biomechanics of the inner foot, like the stress distribution in bones and soft tissue, and the contact pressure at the joints [8] .

The development of FE models arises with the capability of surpass some of the limitations inherent to cadaveric studies. FE modelling and analysis has become an increasingly important tool, as computational resources become more powerful, and data handling algorithms become more sophisticated. It has shown to be an effective tool in predicting musculoskeletal function and changes in performance with injury or surgical procedures [9] .

The need for report the stress patterns of the foot to allow a better understanding and prevention of some diseases such as diabetes and leprosy led to the necessity of develop foot and ankle FE models. The first reported study was published in 1981 [10] ,in which a 2D model for the soft tissues of foot's plantar aspect, including muscles, fascia and skin as well as a modelled foam sole was developed with the goal of documenting the stress distribution in the diabetic foot. However, the model didn't' contemplate bony structures, as they were only included years later, in 1983, by Patit et. al [11] who developed a simplified foot model to study the regions of high stresses during three different gait cycle positions: mid-stance, heel strike and push-off positions.

These two models marked the beginning of FE foot and ankle modelling, but they were very simplified 2D models with a significant lack of complexity. The need to develop more realistic models led to the development of the first 3D foot model in a work conducted by Jacob et al. [12] in 1995.

Despite the increase in complexity with the development of a 3D foot model, the existing models still lack complexity both in the anatomical and mechanical point of view. The first 3D finite element model of a normal foot structure, including bones,

ligaments and cartilages was developed by Gefen et al. [13] in 2000.

Five years later, Cheung et al. [14] included in his model bones, cartilages, ligaments and plantar fascia, as well as a soft tissue capsule. The evaluation of the plantar pressure and the internal load transfer between bones during standing, were the main focus of this study that aimed to understand the formation of foot ulcers, that occur commonly in diabetic patients

Most of the papers regarding FE models of flatfoot, simulate the deformity from a healthy subject by releasing some tendons and ligaments. To the author's best knowledge, the first FE flatfoot reconstructed from data relative to a patient with diagnosed flatfoot was proposed by Lewis [15] in his dissertation. The goal of his work was to develop a procedure for creating 3D subject-specific computational models of the foot for analysing the mechanisms of orthopaedic surgeries with special focus on AAFD. The FE model was constituted by eleven bony segments, 65 ligaments, a representation of the plantar fascia and a platform simulating the ground. Finally, different surgeries for AAFD correction were simulated: 1st metatarsal-cuneiform arthrodesis, naviculocuneiform arthrodesis, talonavicular arthrodesis, medial column arthrodesis, subtalar arthrodesis and a medializing calcaneal osteotomy.

In 2014, Wang et. al [16] developed a FE flatfoot model with the aim to be used in future studies to simulate surgical procedures and further realize tailor-made surgeries for individual patients. As in the work from Lewis, the bony structure of the flatfoot was obtained from CT images of a patient diagnosed with AAFD. The model contained 17 bones, 62 ligaments, 9 tendons and the plantar fascia.

The results found that the higher stress areas appeared in the rearfoot, midfoot and forefoot in the simulation but were mostly concentrated in the rearfoot area in the measurements. Additionally, the peak stresses were found to be in a range of the peak stresses reported for healthy feet but smaller than those published for the flatfoot.

In the next year, Wang et. al [17] proposed a FE model for flatfoot consisting of 27 bone segments, 63 ligaments, plantar fascia and soft tissue for use in surgical simulations to improve individualized treatments. The bones and the encapsulated soft tissue were reconstructed from CT images and ligaments and plantar fascia were added manually to the model. A ground plate was also added to the model to simulate the ground effect. Three simulations were perfomed: a normal balanced standing before surgical correction, a surgical correction of medializing calcaneal osteotomy and a surgical correction of lateral column lengthening.

3. Methods

3.1. Image Acquisition and Segmentation

The process of developing a 3D FE model of any anatomical structure starts with the acquisition of the medical image that will be used to define the 3D geometry of the tissues involved. In this case, a weight-bearing CT of a left foot of a 44-year-old male with healthy feet was used to obtain the geometry of the foot without deformity and a weight-bearing CT of a right foot of a 58-year-old female diagnosed with AAFD was used to obtain the geometry of the flatfoot. The segmentation of these images was performed in the open source software ITK-SNAP (version 3.8.0, 2019) [18] .This software implements the active contour method for the segmentation, a semi-automatic approach which combines the efficiency and repeatability of automatic segmentation with human expertise, since the user must specify the initial contour, balance the various forces which act upon it, as well as monitor the evolution.

A region of interest (ROI) was defined, containing only the structure which is going to be segmented. After defining the ROI, an interface is presented where the input image must be converted into an image that is bright in the regions where the contour should expand, dark in the regions where it should be still and bright blue in the regions where it should retract [19] .

In the end of the segmentation, a final manual segmentation was carried out to include in the model the low-density bone regions of tibia and fibula and to refine some boundaries of the other bones segmented.

The surface mesh generated by ITK-SNAP presents a stair-step shape surface that doesn't correspond to the real surface curvature as well as an excess of nodes and faces that do not express relevant information. For this reason, an adjustment in the mesh was done using a smoothing technique. MeshLab [20] was the software used for that purposed, where a Laplacian Smoothening filter was applied to the mesh generated in the segmentation process, since it is commonly used as an effective filter to amend the stair-step-like artifacts, improving the mesh surface.

3.2. Cartilage Modelling

Although cartilages can also be segmented through the same process described before, CT scans aren't the image modality most suitable for this purpose since it is almost impossible to distinguish bone tissue from cartilage. Thus, SolidWorks® was used to virtually simulate the cartilages of the model.

Five cartilages were modelled: tibio-talar cartilage, connecting the inferior surface of the tibia and the superior surface of the talus; tibio-fibular cartilage, connecting the lateral surface of the tibia and the

medial surface of the fibula; calcaneo-talar cartilage, connecting the calcaneus and the talus bone; the last

ones were added to make the connection between the calcaneus and the midfoot and forefoot regions and the talus and that same region.

The final models after inserting the cartilages were exported from SOLIDWORKS® as .parasolid files and imported to ABAQUS® (Dassault Systèmes Simulia Corp., USA).

3.3. Ligament Insertion

Given the difficulty of discriminating ligaments and tendons from the surrounding tissue in CT images, they were manually modelled in ABAQUS®.

There are many ligaments and tendons that support the foot and ankle complex but, for this study, only 4 ligaments and 2 tendons were considered since they were the most significant for the pathology according to the literature. Spring ligament (SL), short plantar ligament (SPL), long plantar ligament (LPL) and deltoid ligament (DL) were added to the model. The deltoid ligament can be divided into four individual parts: tibionavicular (TN) part, tibiocalcaneal (TC) part, posterior tibiotalar (PTi) part and anterior tibiotalar part (ATi). Regarding the tendons, tibialis posterior tendon (TPT) and the Achilles tendon (AT) were modelled. Note that, only the distal part of the Achilles tendon was modelled since the proximal and medial parts were inserted in regions that were not present on the model.

The attachment points of each ligament/tendon were carefully chosen based in anatomical images and bibliographic references and were connected to the bone surface using a continuum distributing coupling constraint. This was done to ensure that the ligament/tendon is attached to the insertion site and that the forces were uniformly distributed on the surface, mimicking what happens in the human body, while avoiding concentration points.

The ligaments/tendons were modelled as tension only truss elements using the “no compression” option defined by ABAQUS®. Additionally, a pre-stretch on 2% was applied to every ligament and tendon to represent *in situ* levels, according to the work of Liacouras et al. [21] .

3.4. Material Properties

Given the complexity of the material properties of biological tissues, for the mechanical properties of bone, cartilage, ligaments, and tendons several approximations had to be considered for the sake of simplicity and to reduce the computational effort.

Bone was considered a linearly elastic, homogenous, and isotropic material, meaning that no difference between cortical and trabecular bone was considered and it is not directionally dependent. A Young’s modulus of 7300 MPa was assigned to bone, selected by weighting cortical and trabecular elasticity values [14] and a Poisson’s ratio of 0,3 was used [22].

Cartilage was also considered as a linearly elastic and isotropic material with a Young’s modulus of 10 MPa and a Poisson’s ration of 0,4 for its nearly incompressible nature [22], [23].

Ligaments and tendons were also considered as linear elastic materials but with different Young’s modulus since they are different materials, but have the same Poisson’s ratio of 0,4. For the ligaments, a Young’s modulus of 264,8 MPa [24] was used and for the tendons the Young’s modulus was considered to be 1500 MPa [16] .Additionally, they were assumed to have different cross sectional areas that were taken from the literature. *Table 2* resumes the material properties of each ligament/tendon as well as the literature references that were used to define them. Note that the cross-sectional area of the plantar ligaments was considered the same since it is very difficult to distinguished them from each other in the measurement trials [25] .

Table 2 - Material properties for ligaments and tendons.

Ligament/Tendon	Young's Modulus (MPa)	Poisson's Ratio	Cross-sectional area (mm2)	Reference
Tibialis Posterior Tendon	1500	0,4	16,10	[26]
Achilles Tendon			84,20	[27]
Spring Ligament	264,8		28,48	[25]
Short Plantar Ligament			58,06	[25]
Long Plantar Ligament			58,06	[25]
Deltoid Ligament				
Tibionavicular Part	264,8	0,4	28,08	[28]
Tibiocalcaneal Part			43,20	[29]
Posterior Tibiotalar Part			78,43	[29]
Anterior Tibiotalar Part			43,49	[29]

3.5. Model Interactions

The interactions between all parts of the models (bones and cartilages) were considered rigidly bonded using the tool merge geometry, selecting the option retain intersecting boundaries. The interaction between the bones and the ligaments were achieved by using a coupling constraint as explained previously.

3.6. Loading and Boundary Conditions

A loading case to simulate a normal standing load position was created with a 375 N descending vertical force, corresponding to half of the body weight of an average individual (75 Kg) leaning on one foot. The load was applied to a reference point (RP) created on the top surface of the tibia and coupled with the top surface of the tibia and the top surface of fibula. This allowed an uniform distribution of the load across the surface. This way, a traditional

AAFD diagnostic assessment scenario is emulated with the patient leaning on one foot [6] .

The ground effect was simulated when an adult individual is leaning on one foot. For that purpose, an *encastre* was performed on the inferior part of the calcaneus as well as a blockage of the vertical displacement on the 1st and 5th metatarsals [6], [30].

For comparison purposes, the same loading and boundary conditions were applied to both foot models.

3.7. Mesh Generation

In this work, bones and cartilages were described by linear tetrahedral (C3D4) elements and ligaments were defined by 2-node linear 3D trusses (T3D2).

For the merged foot containing the bone and the cartilage a mesh size of 2 mm was chosen for both the healthy foot and the flatfoot. Some adjustments using the virtual topology tool were done in both models to avoid problematic regions on the meshes. In the healthy foot a mesh of 270 172 elements was generated, while the mesh generated for flatfoot had 260 864 elements.

The meshing of the ligaments was done using a linear truss mesh with the size equal to the length of the ligament to assure that each ligament was meshed with only one element. So, the ligaments were defined with 14 tension-only truss elements.

In *Figure 1* the meshes generated on each model can be observed.

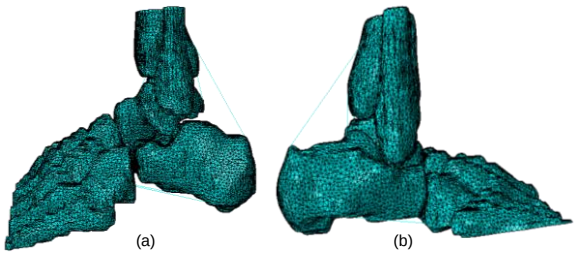

Figure 1 - Meshed foot models. (a) Mesh generated on the normal foot and (b) mesh generated on flatfoot.

4. Results and Discussion

To understand how the stresses are distributed on the foot, von Mises stresses were measured for both the healthy and the flatfoot models (*Figure 2)*.

The von Mises stresses distribution on the healthy foot was the expected, with higher stresses on the inferior region of the calcaneus as well as in the distal regions of the 1st and 5th metatarsals. These results were in agreement with the ones obtained by in his work, since these are the regions that contact with the ground in a balanced standing position for a healthy subject.

The lower stresses were observed for the proximal regions of the 2nd, 3rd and 4th metatarsals as well as for the bases of the 1st and 5th metatarsals.

For the flatfoot, the higher stresses occurred for almost the same regions as in the healthy foot. However, an increase on the stresses acting on the tibia and fibula is observed. These bones are the ones that support the load created by the body weight and are responsible for distributing it through the foot. When the geometry of the foot is altered, such as the flatfoot this load transfer is also altered, leading to a different distribution of the stresses within the foot.

The higher stress region on the calcaneus is bigger than in the healthy foot, probably as a consequence of the flattened arch, which increases the contact area between the foot and the ground. Moreover, these higher stresses regions occur in both models and correspond to the regions where boundary conditions were applied.

Given the importance of the ankle joint on the foot mobility and function, a more detailed evaluation was performed. For that purpose, an individual analysis of the von Mises stresses acting on the calcaneus, talus, fibula and tibia was done.

In general, it was possible to conclude that the bones are more loaded when the foot sets up into a flatfoot state, since the load transfer is altered due to the misalignment of the foot joints that characterize the deformity. This alteration on the transfer of the load through the foot joint is responsible for altering the distribution of the stresses within the foot and joints.

An analysis of the cartilages (*Figure 3 a))* was also performed in this study, to see the alterations on this tissue on both models. An increase of the bon Mises peak stresses occur for most of the cartilages of the flatfoot, comparing with the healthy foot. The only cartilage that suffered a reduction of the von Mises stresses on the flatfoot compared with the healthy foot was the one connecting the talus and the calcaneus. Additionally, this cartilage is the one with the higher peak von Mises stress, occurring for the healthy foot. The discrepancy of the peak von Mises stresses of both models for this cartilage can be a consequence of model limitations.

For the ligaments and tendons (*Figure 3 b))*, an increase in the stresses of the ligaments and tendons of the flatfoot was observed. This was expected because, giving the alterations in the geometry inherent to the deformity, one can expect that the ligaments to be subjected to higher stress values.

On the other hand, the fact that there was a decrease of the tension on the spring ligament, and since it is one of the most affected on the deformity, one can conclude that it can be already affected on this patient.

Some structures yield 0 stresses values probably because they were compressed instead of stretch.

However, since the “no compression” option was chosen this cannot happen on the models. Note that most of these 0 stresses values occur for the TN, TC, PTi and ATi of the flatfoot. These ligaments are part of the deltoid ligament, which is strongly affected by this deformity. As explained for the SL, these values may mean that the DL could be already affected on the patient in study.

the flatfoot was subject to higher stresses than the healthy. However, the peak von Mises stress occurred for the healthy foot probably due to limitations on the development of the FE model. Concerning the cartilages, it was possible to conclude that, in the flatfoot the peak of von Mises stresses was increased comparing with the healthy foot, due to the altered load transfer provoked by the misalignment of the foot joints that characterized the

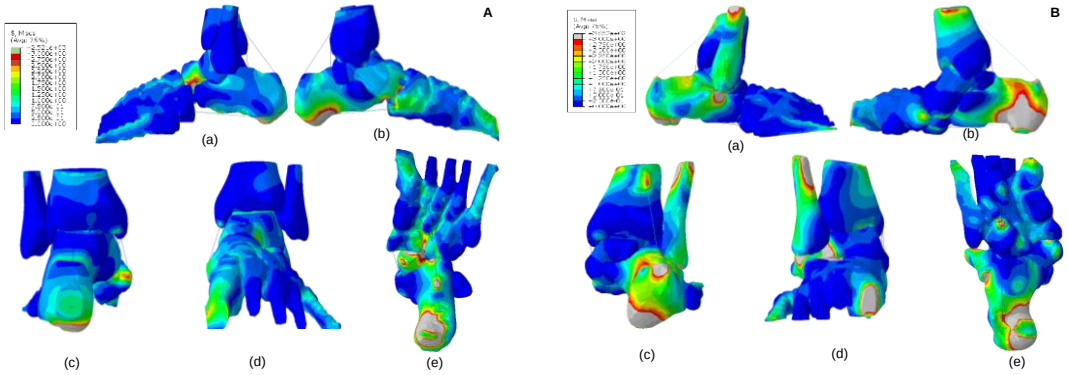

Figure 2 – von Mises stresses distributions on the healthy foot (A) and flatfoot (B). (a) lateral view, (b) medial, (c) posterior view, (d) anterior view and (e) plantar view.

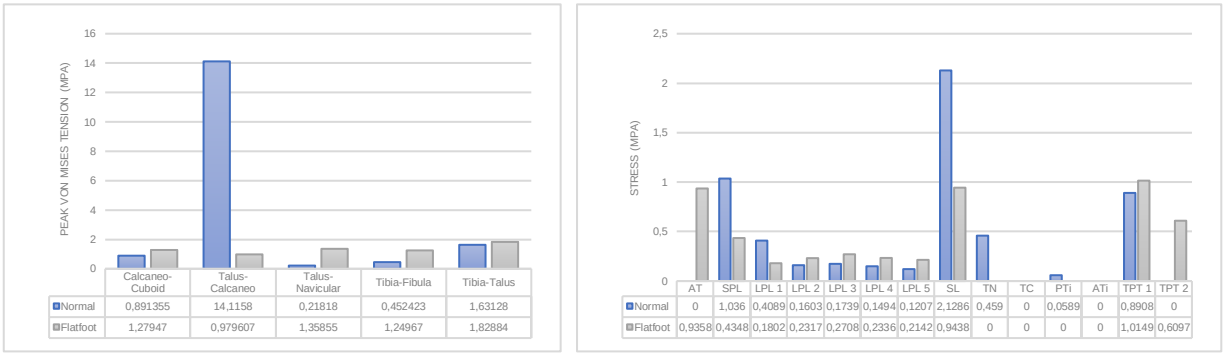

Figure 3 – Peak von Mises stresses for the cartilages (a) and ligaments/tendons (b) for the healthy foot (blue) and flatfoot (grey).

5. Conclusion and Future Work

The aim of this study was to create a FE model of both a healthy foot and a flatfoot that was able to predict, by comparing both models, the biomechanical alterations of the foot when its anatomy sets up in a deformed situation.

A FE model for both a healthy foot and a flatfoot was developed comprising bones, cartilages, ligaments, and tendons. The geometry of the bones was obtained through CT images of a healthy and a diagnosed flatfoot and the boundary and loading conditions were taken from the literature and previous studies.

A comparison between the von Mises stresses distribution of the healthy and the flatfoot was done for the entire foot as well as for the individualized bones that made up the ankle joint. Additionally, von Mises stresses of cartilages, ligaments and tendons were also targeted. Overall, the results showed that deformity.

The results obtained in the study of the ligaments and tendons allowed to conclude that the majority of the ligaments and tendons of the flatfoot were more tensioned than the ones of the healthy foot. Additionally, some of them yield 0 stress values, meaning that they could be under compression instead of tension, since the “no compression” option was used. On the other hand, the results obtained for the spring and deltoid ligaments could mean that these ligaments were already affected on the patient studied on this work.

It is important to mention that, to the author’s best knowledge, this is the first FE study on the literature that studies the biomechanical alterations of a flatfoot compared with a healthy foot.

This thesis could be the starting point for further investigation about the internal biomechanics of the flatfoot, contributing for a better understanding of the

deformity and, consequently, an improvement of the treatment options. Nevertheless, the models have some limitations which should be addressed to create a more outright representation of the foot and ankle complex, thus being able to better represent and reproduce *in vivo* conditions.

The main limitation has to do with the mechanical properties used in this work. This is because bone, cartilage, and ligaments/tendons, were modelled as linear elastic, isotropic and homogenous, when in fact they possess other mechanical characteristics. For more realistic biological conditions, future studies should include a differentiation between cortical and trabecular bone. On the other hand, for the cartilages, ligaments and tendons anisotropic and viscoelastic material properties should be used [49] . Moreover, ligaments and tendons should be modelled with more than one truss since they are composed of multiple collagen fibres and not of one single fibre [6].

A second limitation concerns the loading and boundary conditions used on the work. A balanced standing position was simulated with only the body weight acting upon it. In the future, simulations under different stance phases as well as adding the role of muscles forces could lead to more realistic models and more accurate conclusions.

Another limitation is the fact that the conclusions were taken based on only one AAFD patient. In the future, more patients should be analysed, in different stages of the deformity, to allow a better prediction of the results.

Finally, further investigation is required addressing the limitations described above and, in the future, the model should be used to assess the different treatment options by performing them computationally. This way, the long-term effects on the biomechanics of the foot could be assessed and, hopefully, this work will contribute to the development of an optimal surgery plan and a tailor-made surgery for individual patients.

6. Acknowledgements

This document was written and made publically available as an institutional academic requirement and as a part of the evaluation of the MSc thesis in Biomedical Engineering of the author at Instituto Superior Técnico. The work described herein was performed at the Mechanical Engineer Department (DEM) of Instituto Superior Técnico (Lisbon, Portugal), during the period March-December 2020, under the supervision of Prof. Paulo Fernandes and Prof. João Folgado.

7. References

[1] S. N. K. K. Arachchige, H. Chander, and A. Knight, “The Foot Flat feet : Biomechanical implications , assessment and management,” *Foot*, vol. 38, no. January, pp. 81–85, 2019.

[2] E. Vulcano, J. T. Deland, and S. J. Ellis, “Approach and treatment of the adult acquired flatfoot deformity,” no. Table 1, pp. 6–8, 2013.

[3] M. C. Alley, R. Shakked, and A. J. Rosenbaum, “Adult-Acquired Flatfoot Deformity,” vol. 5, no. 8, pp. 1–11, 2017.

[4] N. A. Smyth, A. A. Aiyer, J. R. Kaplan, C. A. Carmody, and A. R. Kadakia, “Adult-acquired flatfoot deformity,” *Eur. J. Orthop. Surg. Traumatol.*, 2017.

[5] D. V. Flores, C. M. Gómez, M. F. Hernando, M. A. Davis, and M. N. Pathria, “Adult acquired flatfoot deformity: Anatomy, biomechanics, staging, and imaging findings,” *Radiographics*, vol. 39, no. 5, pp. 1437–1460, 2019.

[6] C. Cifuentes-De la Portilla, R. Larrainzar-Garijo, and J. Bayod, “Analysis of the main passive soft tissues associated with adult acquired flatfoot deformity development: A computational modeling approach,” *J. Biomech.*, vol. 84, pp. 183–190, 2019.

[7] Z. Wang, M. Kido, K. Imai, K. Ikoma, and S. Hirai, “Engineering Towards patient-specific medializing calcaneal osteotomy for adult flatfoot : a finite element study,” *Comput. Methods Biomech. Biomed. Engin.*, vol. 5842, pp. 1–12, 2018.

[8] I. Division, B. Engineering, H. Hom, and H. K. Sar, “Computational Models of the Foot and Ankle for Pathomechanics and Clinical Applications : A Review,” 2015.

[9] K. Hollerbach, A. Hollister, and E. Ashby, “3-D Finite Element Model Development for Biomechanics: a Software Demonstration,” *Sixth Int. Symp. Comput. Simul. Biomech.*, 1997.

[10] S. Nakamura, R. D. Crowninshield, and R. R. Cooper, “An analysis of soft tissue loading in the foot - A preliminary report,” *Bull. Prosthet. Res.*, vol. 18, no. 1, pp. 27–34, 1981.

[11] K. M. Patil, L. H. Braak, and A. Huson, “Stresses in a simplified two dimensional model of a normal foot - A preliminary analysis,” *Mech. Res. Commun.*, vol. 20, no. 1, pp. 1–7, 1993.

[12] S. Jacob, K. M. Patil, L. H. Braak, and A. Huson, “Three dimensional two arch model of a normal foot for stress analysis,” *IEEE/ Eng. Med. Biol. Soc. Annu. Conf.*, pp. 23–24, 1995.

[13] A. Gefen, M. Megido-Ravid, Y. Itzchak, and M. Arcan, “Biomechanical analysis of the three-dimensional foot structure during gait: A basic tool for clinical applications,” *J. Biomech. Eng.*, vol. 122, no. 6, pp. 630–639, 2000.

[14] J. T. M. Cheung, M. Zhang, A. K. L. Leung, and Y. B. Fan, “Three-dimensional finite element analysis of the foot during standing - A material sensitivity study,” *J. Biomech.*, vol. 38, no. 5, pp. 1045–1054, 2005.

[15] G. S. Lewis, “Computational modeling of the mechanics of flatfoot deformity and its surgical corrections,” no. December, p. 119, 2008.

[16] Z. Wang, K. Imai, M. Kido, K. Ikoma, and S. Hirai, “A finite element model of flatfoot (Pes Planus) for improving surgical plan,” *2014 36th Annu. Int. Conf. IEEE Eng. Med. Biol. Soc. EMBC 2014*, vol. m, pp. 844–847, 2014.

[17] Z. Wang, K. Imai, M. Kido, K. Ikoma, and S. Hirai, “Study of Surgical Simulation of Flatfoot Using a Finite Element Model,” vol. 45, pp. 353–363, 2016.

[18] P. A. Yushkevich *et al.*, “User-guided 3D active contour segmentation of anatomical structures : Significantly improved efficiency and reliability,” vol. 31, pp. 1116–1128, 2006.

[19] P. Yushkevich, J. Piven, H. Cody, and S. Ho, “User-guided level set segmentation of anatomical structures with ITK-SNAP,” *Neuroimage*, vol. 31, no. 3, pp. 1116–1128, 2006.

[20] P. Cignoni, M. Callieri, M. Corsini, M. Dellepiane, F. Ganovelli, and G. Ranzuglia, “MeshLab: An open-source mesh processing tool,” *6th Eurographics Ital. Chapter Conf. 2008 - Proc.*, pp. 129–136, 2008.

[21] P. C. Liacouras and J. S. Wayne, “Computational modeling to predict mechanical function of joints: Application to the lower leg with simulation of two cadaver studies,” *J. Biomech. Eng.*, vol. 129, no. 6, pp. 811–817, 2007.

[22] G. Marta, C. Quental, and J. Folgado, “Computational study of contact patterns in the ankle joint after ligamentous injury Gonc Biomedical Engineering,” no. October, 2018.

[23] C. Xu, M. Li, C. Wang, and H. Liu, “Nonanatomic versus anatomic techniques in spring ligament reconstruction : biomechanical assessment via a finite element model,” vol. 5, pp. 5–7, 2019.

[24] D. W. C. Wong, Y. Wang, A. K. L. Leung, M. Yang, and M. Zhang, “Finite element simulation on posterior tibial tendinopathy: Load transfer alteration and implications to the onset of pes planus,” *Clin. Biomech.*, vol. 51, no. June 2017, pp. 10–16, 2018.

[25] K. H. Schmidt and W. R. Ledoux, “Quantifying ligament cross-sectional area via molding and casting,” *J. Biomech. Eng.*, vol. 132, no. 9, pp. 1–6, 2010.

[26] S. Park, J. Lee, H. R. Cho, K. Kim, Y. S. Bang, and Y. U. Kim, “The predictive role of the posterior tibial tendon cross-sectional area in early diagnosing posterior tibial tendon dysfunction,” *Medicine (Baltimore).*, vol. 99, no. 36, p. e21823, 2020.

[27] S. Bohm, F. Mersmann, A. Schroll, N. Mäkitalo, and A. Arampatzis, “Insufficient accuracy of the ultrasound-based determination of Achilles tendon cross-sectional area,” *J. Biomech.*, vol. 49, no. 13, pp. 2932–2937, 2016.

[28] J.-F. Zhu *et al.*, “A new ligament cross-sectional area measuring instrument: Design and application,” *Chinese J. Tissue Eng. Res.*, vol. 20, pp. 7654–7659, 2016.

[29] C. Mkandawire, W. R. Ledoux, B. J. Sangeorzan, and R. P. Ching, “Foot and ankle ligament morphometry,” *J. Rehabil. Res. Dev.*, vol. 42, no. 6, pp. 809–819, 2005.

[30] C. Cifuentes-de, R. Larrainzar-garijo, and J. Bayod, “Foot and Ankle Surgery Analysis of biomechanical stresses caused by hindfoot joint arthrodesis in the treatment of adult acquired fl atfoot deformity : A fi nite element study,” *Foot Ankle Surg.*, 2019.

[31] S. C. Tadepalli, A. Erdemir, and P. R. Cavanagh, “Comparison of hexahedral and tetrahedral elements in finite element analysis of the foot and footwear,” *J. Biomech.*, vol. 44, no. 12, pp. 2337–2343, 2011.